PHYSICAL REVIEW B **91**, 121404(R) (2015)

Observation of vacancy-induced suppression of electronic cooling in defected graphene

Qi Han,* Yi Chen,* Gerui Liu, Dapeng Yu, and Xiaosong Wu†
State Key Laboratory for Artificial Microstructure and Mesoscopic Physics, Peking University, Beijing 100871, China and Collaborative Innovation Center of Quantum Matter, Beijing 100871, China
(Received 1 August 2014; revised manuscript received 6 February 2015; published 6 March 2015)

Previous studies of electron-phonon interaction in impure graphene have found that disorder can give rise to an enhancement of electronic cooling at high temperatures. We investigate the effect of lattice vacancy in both mono- and bilayer graphene and observe an order of magnitude suppression of electronic cooling at low temperatures compared with clean graphene. The dependence of the coupling constant on the phonon temperature implies its link to the dynamics of disorder. Our study highlights the effect of disorder on electron-phonon interaction in graphene. In addition, the suppression of electronic cooling holds great promise for improving the performance of graphene-based bolometer and photodetector devices.

DOI: 10.1103/PhysRevB.91.121404 PACS number(s): 72.80.Vp, 63.22.Rc

I. INTRODUCTION

In recent years, there has been considerable interest in utilizing graphene as photodetectors [1–8]. Most of these detectors are based on a hot electron effect, i.e., the electronic temperature being substantially higher than the lattice temperature. Two properties of graphene strongly enhance the effect. First, low carrier density gives rise to a very small electron specific heat. Second, weak electron-phonon (e-p) interaction reduces the heat transfer from the electron gas to the lattice. Thus, it is of practical interest to understand the e-p interaction in graphene. Both theoretical and experimental efforts have been devoted to this topic. Earlier work was mainly focused on clean graphene and considered the Dirac spectrum of electrons [9–15]. As the important role of impurities in electronic transport has been revealed, its effects on the e-p interaction began to draw attention [16–18]. For instance, due to the chiral nature of electrons, long-range and short-range potentials scatter electrons differently in graphene [19–21]. Recently, a strong enhancement of electronic cooling via e-p interaction in presence of short-range disorder has been predicted [18]. This is achieved via a so-called supercollision process. When the carrier density is low, the Bloch-Grüneisen temperature T_{BG} can be quite small. Since T_{BG} sets the maximum wave vector of phonons that can exchange energy with electrons, when $T > T_{BG}$, only a portion of phonons can contribute to the energy relaxation. Interestingly, in the presence of short-range potentials, the theory has found that a disorder-assisted scattering process can occur, in which all available phonons are able to participate. As a result, the energy relaxation is strongly enhanced. Recently, it has been experimentally confirmed [22–24]. Supercollision takes place at high temperatures; it would be interesting to see how disorder affects the e-p interaction when $T < T_{BG}$.

Here, we present an experimental investigation of the effect of vacancy on electronic cooling at $T < T_{BG}$ in both monolayer and bilayer defected graphene. By studying the nonlinear electric transport of defected graphene, a strong *suppression* of e-p energy relaxation, instead of an *enhancement* in the case of static potentials, has been observed. Our work provides experimental insight on the effect of scattering potential on e-p interaction. Moreover, the suppression suggests that the performance of graphene hot electron photodetectors can be further improved by introducing vacancies.

II. EXPERIMENT

In this work, we have investigated four exfoliated graphene samples on Si/SiO_2 substrates. The thickness of all the monolayer (SM1 and SM2) and bilayer (SB1 and SB2) samples were estimated by optical contrast and confirmed by Raman spectroscopy [25]. Graphene flakes were patterned into ribbons, using e-beam lithography. 5-nm Ti/80-nm Au were e-beam deposited, followed by lift-off to form electrodes. Typical sample geometry can be seen in the inset of Fig. 1(a). In order to introduce vacancies, samples were then loaded into a Femto plasma system and subject to argon plasma treatment for various periods (from 1 to 5 s) [26]. Four-probe electrical measurements were carried out in a cryostat using a standard lock-in technique. Room temperature π filters were used to avoid heating of electrons by radio frequency noise. The information for four samples is summarized in Table I.

III. RESULTS AND DISCUSSION

Previously, we have already demonstrated a hot electron bolometer based on disordered graphene [27]. It has been shown that the divergence of the resistance at low temperature can be utilized as a sensitive thermometer for electrons. By applying Joule heating, the energy transfer rate between the electron gas and the phonon gas can be obtained. The same method has been employed in this work. As shown in Fig. 1(a), the resistance of defected graphene exhibits a sharp increase as the temperature decreases (data for the bilayer sample SB1 can be found in the Supplemental Material [28]). The divergence becomes stronger as one approaches the charge neutrality point (CNP). The $R - T$ behavior can be well fitted to variable range hopping transport, described as $R \propto \exp[(T_0/T)^{1/3}]$ [29]. Here, the characteristic temperature $T_0 = 12/[\pi k_B \nu(E_F)\xi^2]$, with k_B the Boltzmann constant, $\nu(E_F)$ the density of states at the Fermi level E_F, and ξ the localization length. By fitting

*These two authors contributed equally.
†xswu@pku.edu.cn

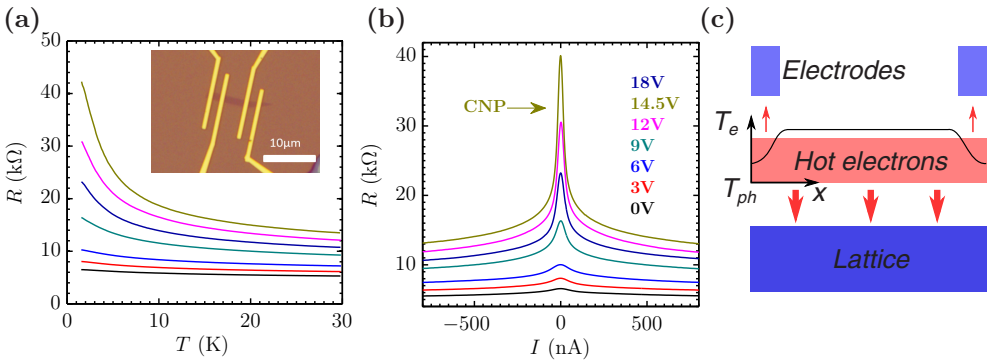

FIG. 1. (Color online) Resistance of defected graphene. (a) Temperature dependence of resistance in sample SM1 at different gate voltages, showing divergence at low temperature. Inset: Optical micrograph of a typical device configuration. (b) Resistance of SM1 as a function of Joule heating current at different gate voltages at $T = 1.5$ K. The CNP is at 14.5 V. (c) Thermal model for the structure. The pathways of heat dissipation are indicated by red arrows.

to this formula, the localization length ξ is determined. It is employed as a measure of the degree of disorder. ξ near the CNP for all samples are listed in Table I.

In steady Joule heating, the electron cooling power is equal to the heating power. The corresponding thermal model is sketched in Fig. 1(c). Two thermal energy transfer pathways are indicated, i.e., via electron diffusion into electrodes or e-p interaction into the lattice. In our strongly disordered graphene, the former is significantly suppressed due to a very low carrier diffusivity and e-p interaction dominates the energy dissipation (see the Supplemental Material for a detailed analysis of the thermal model [28]). Then, the electronic temperature can be directly inferred from the resistance. Furthermore, it is estimated that the thermal conductance between the graphene lattice and the substrate is much higher than that due to e-p interaction. Thus, the phonon temperature $T_{\rm ph}$ is approximately equal to the substrate temperature T [5,22,30]. Under these conditions, the energy balance at the steady state of Joule heating can be written as

$$P = A\left(T_{\rm e}^{\delta} - T_{\rm ph}^{\delta}\right), \tag{1}$$

where P is the Joule heating power, A is the coupling constant, and $T_{\rm e}$ is the electronic temperature. δ ranges from 2 to 6, depending on the details of the e-p scattering process [12].

Upon Joule heating, the electronic temperature is raised, leading to a decrease of the resistance, depicted in Fig. 1(b). Based on the resistance as a function of temperature, we obtain the $P - T_{\rm e}$ relation at different carrier densities, plotted in the insets of Fig. 2. P is also plotted against $T_{\rm e}^3 - T_{\rm ph}^3$. The linear behavior agrees well with Eq. (1) with $\delta = 3$ for both monolayer and bilayer graphene at all carrier densities. It has been theoretically shown that both clean monolayer and bilayer graphene can be described by Eq. (1) with $\delta = 4$ at low temperature [9,12]. In the presence of disorder, e-p interaction is enhanced and δ is reduced to 3 [17,18]. δ obtained in our result is consistent with these theories, indicating the effect of defects. T^3 dependence has also been reported in some other experiments. In the following, we will compare our results in detail with previous theoretical and experimental results.

The e-p interaction is usually considered in two distinct regimes: high temperature and low temperature. In normal metals, Debye temperature $\theta_{\rm D}$ demarcates two regimes. Below $\theta_{\rm D}$, the phase space of available phonons increases with temperature, while it becomes constant above it (all modes are excited). In graphene, because of its low carrier density, the Bloch-Grüneisen temperature $T_{\rm BG}$ becomes the relevant characteristic temperature. It is defined as $2k_{\rm B}T_{\rm BG} = 2hck_{\rm F}$. Here $k_{\rm B}$ is the Boltzmann constant, h is the Plank constant, c is the sound velocity of graphene, and $k_{\rm F}$ is the Fermi wave vector. $T_{\rm BG}$ stems from the momentum conservation in e-p scattering. Because of it, when $T_{\rm ph} > T_{\rm BG}$, only a portion of the phonons can participate in the process [31]. Considering the band structure of graphene, we have $T_{\rm BG} = 2(c/v_F)E_{\rm F}/k_{\rm B}$ in

TABLE I. Sample information of four investigated devices. $V_{\rm CNP}$ is the charge neutrality point (CNP) of samples and ξ is the localization length near the CNP.

Devices	Length (μm)	Width (μm)	$V_{\rm CNP}$ (V)	ξ (nm)
SM1	2	3	14.5	156
SM2	6.7	2.7	30	21
SB1	3	2.7	70	50
SB2	6	2.7	57	54

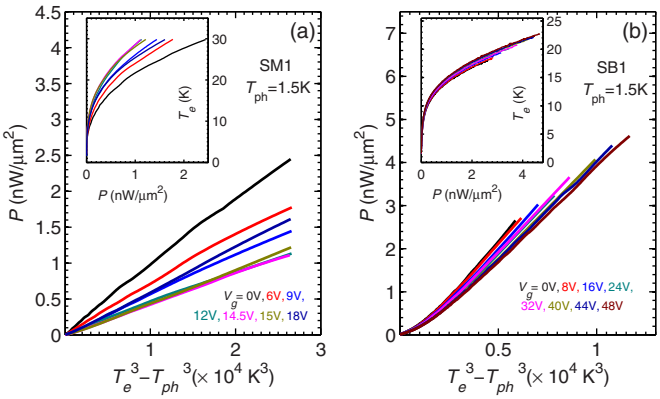

FIG. 2. (Color online) Cooling power of monolayer and bilayer defected graphene. (a), (b) Cooling power P against $T_{\rm e}^3 - T_{\rm ph}^3$ shows a linear dependence for both monolayer and bilayer samples. Inset: P versus $T_{\rm e}$.

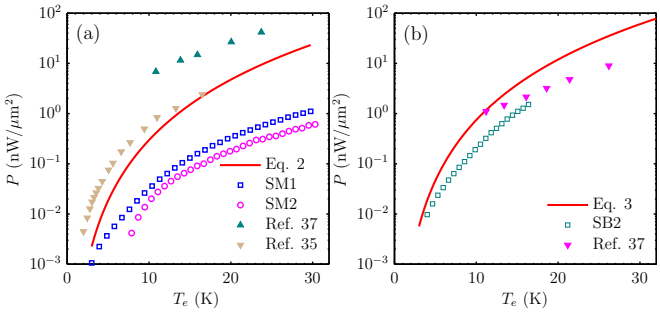

FIG. 3. (Color online) Suppression of electronic cooling in defected graphene. (a) Cooling power of monolayer graphene. The solid line is a plot of Eq. (2) for clean graphene at $n = 4 \times 10^{11}$ cm^{-2}. The solid symbol represents experiment results of pristine graphene from others' work. The up triangle represents data from [37] at $n = 4 \times 10^{11}$ cm^{-2} and $T_{ph} = 1.8$ K, while the down triangles represent data from [35] at $n = 2.2 \times 10^{12}$ cm^{-2} and $T_{ph} = 0.8$ K. The open symbol represents our data. n_0 is 4×10^{11} cm^2 to account for charge puddles near CNP. T_{ph} is 1.5 K in SM1 and 7 K in SM2. (b) Cooling power of bilayer graphene. The solid line is a plot of Eq. (3) for clean graphene at $n = 2.8 \times 10^{12}$ cm^{-2} and $T_{ph} = 1.5$ K. The solid symbol represents experiment results of pristine graphene at $n = 2.7 \times 10^{12}$ cm^{-2} and $T_{ph} = 1.8$ K, taken from [37]. The open symbol depicts our results for SB2 at $n = 2.8 \times 10^{12}$ cm^{-2} and $T_{ph} = 1.5$ K. The data for SB1 (not shown) almost overlap SB2.

monolayer graphene and $T_{BG} = 2(c/v_F)\sqrt{\gamma_1 E_F}/k_B$ in bilayer graphene [12]. Here $v_F \approx 10^6$ m/s is the Fermi velocity, $c \approx 2 \times 10^4$ m/s, and $\gamma_1 \approx 0.4$ eV is the interlayer coupling coefficient. Taking into account a residual carrier density $n_0 \approx 4 \times 10^{11}$ cm^2 due to charge puddles [32,33], it can be readily estimated that even at the CNP, $T_{BG} > 34$ K. It is much higher than $T_e = 1.5$ K in our experiment. Consequently, we are well in the low temperature regime.

In the low temperature regime, the whole population of phonons can interact with electrons. Thus, the disorder-assisted supercollision is negligible [18], which rules it out as the origin of the observed T^3 dependence. It has been theoretically shown that in the case of weak screening, static charge impurities leads to enhanced e-p cooling power over clean graphene and $\delta = 3$ [17]. For comparison, we plot our data, the theoretical cooling power of clean graphene, in Fig. 3. The theoretical prediction of the cooling power per unit area in clean monolayer graphene is [12]

$$P_{clean} = \frac{\pi^2 D^2 E_F k_B^4}{15\rho\hbar^5 v_F^3 c^3}\left(T_e^4 - T_{ph}^4\right), \tag{2}$$

where $\rho \approx 0.76 \times 10^{-6}$ kg/m^2 is the mass density of graphene and D is the deformation potential chosen as a common value 18 eV [23,34,35] (this choice will be discussed later). The theoretical cooling power P_{clean} as a function of the electron temperature at $n = 4 \times 10^{11}$ cm^{-2} and $T_{ph} = 1.5$ K is plotted in Fig. 3(a). It can be clearly seen that the cooling power of our disordered samples SM1 and SM2 is over an order of magnitude smaller [36]. Similar suppression is observed at all carrier densities. For comparison, we also plot the data from two other experiments in which T^3 dependence was observed at low temperatures [35,37]. These results (with similar T_{ph}) are above the theoretical curve. For the more disordered sample, SM2, the suppression is even stronger.

Similar suppression occurs in bilayer graphene samples, too. The cooling power per unit area in clean bilayer graphene is given by [12]

$$P_{clean} = \frac{\pi^2 D^2 \gamma_1 k_B^4}{60\rho\hbar^5 v_F^3 c^3}\sqrt{\frac{\gamma_1}{E_F}}\left(T_e^4 - T_{ph}^4\right). \tag{3}$$

Figure 3(a) shows the plot of Eq. (3), the cooling power of the bilayer samples SB1 and SB2, and the data from [37]. Although not as pronounced as monolayer graphene, our data are still below the theoretical surface. The weaker suppression may result from the fact that the bottom layer of bilayer graphene has experienced less damage by our low energy plasma than the top one [26]. Therefore, this less disordered layer provides a channel of substantial cooling.

The e-p coupling strength depends on the deformation potential D, which characterizes the band shift upon lattice deformation [38–40]. For the theoretical cooling power surface in Fig. 3, we use $D = 18$ eV. Note that D for graphene ranges from 10 to 70 eV in various experiments, but 18 eV is the most common value for graphene [35]. If the suppression is due to an overestimated D, to account for the small cooling power, one would require D to be only about 5 eV, one-half of the lowest value reported. Therefore, we believe that the suppression cannot be explained by a small D.

By linear fits of P versus $T_e^3 - T_{ph}^3$, the coupling constant A can be obtained. In Fig. 4, A is plotted as a function of carrier density n. A for all samples decreases when approaching the CNP. This is because fewer carriers at Fermi level could contribute to the total cooling power.

We now take a look at the dependence of the coupling constant on the degree of disorder. The degree of disorder is indicated by the localization length ξ. For instance, ξ for SM1 and SM2 is 156 and 21 nm, respectively. Consequently, the coupling constant A of SM1 is only about one-third of the value of SM2, as depicted in Fig. 4(a). The dependence of A on ξ is consistent with the suppression of the e-p scattering by disorder. For the two bilayer samples, SB1 and SB2, the localization lengths are close. The n dependence of A for both samples aligns reasonably well and is consistent with the monolayer samples [see Fig. 4(b)].

The Joule heating experiment has also been carried out at different phonon temperatures T_{ph}. In Fig. 4(c), the coupling constant A is plotted as a function of T_{ph}. Usually, A is independent of T_{ph}, which is actually seen at low temperature for SB1. However, as the temperature goes above 7 K, A is enhanced. Later, we will show that the unexpected T dependence is likely related to the dynamic nature of vacancies.

At first glance, the suppression of electronic cooling by vacancies seems surprising, in that the theory has predicted that in the Bloch-Grüneisen regime, disorder would enhance the cooling [17]. Earlier experimental results have confirmed it [35,37]. There is one exception in which weaker cooling was found for a more disordered sample [13]. However, it is not clear what kind of disorder dominated electronic scattering in the sample. It will be shown that the nature of disorder might play a critical role in the electronic cooling. The difference

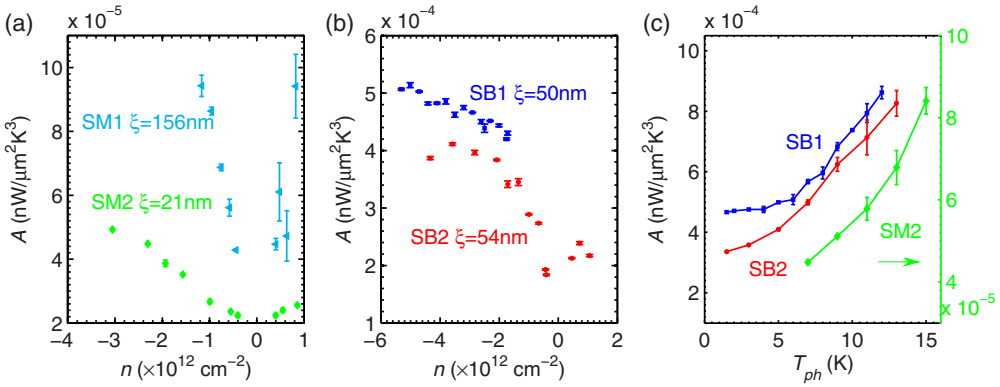

FIG. 4. (Color online) Coupling constant A. (a) Extracted coupling constant A as a function of carrier density n in monolayer samples. (b) Dependence of A on carrier density n in bilayer graphene samples. The curves for two samples with similar degree of disorder align reasonably well, confirming the consistency of our experiment. (c) Dependence of A on phonon temperature $T_{\rm ph}$. The data of SM2 are plotted with respect to the right y axis. The error bar reflects the difference of A obtained by the nonlinear IV at the positive bias and negative bias.

between our samples and others is that the dominant disorder is the vacancy instead of the charge impurity. One possibility is that the suppression is caused by the change of the density of states (DOS) due to vacancies. It has been found that vacancies lead to an enhancement of DOS around the Dirac point [41]. An increase of the phase space often strengthens e-p scattering, which is the opposite of what we have observed. Moreover, the change of DOS occurs only in the vicinity of the Dirac point, while the observed suppression smoothly extends to high carrier density. Thus, the effect of DOS can be ruled out.

The effect of disorder on the e-p interaction has been extensively studied in disordered metals. The experimental results were mixed, as both enhancement and suppression of the e-p coupling have been observed [42–45]. It was realized that the effect depends on the character of disorder [46–49]. Static disorder prolongs the effective interacting time between an electron and a phonon, leading to an enhancement of interaction. The power index δ in Eq. (1) decreases by one. In contrast, dynamic disorder (disorder that is completely dragged by phonon) modifies the quantum interference of scattering processes [47], suppressing the interaction, in accordance with the famous Pippard's ineffectiveness condition [50]. δ often increases by one. To see the suppression, dynamic disorder scattering has to be the dominant one, otherwise a small amount of static disorder will reverse the effect [47].

Apparently, our samples satisfy the condition, as vacancies are the dominant scatterers and also completely dragged by phonons. We speculate that suppression of e-p interaction is due to dynamic disorder. In previous studies, disorder is theoretically considered to be static. This is also true in other experimental work, in which the dominant disorder is due to charge impurities [51,52]. The difference in the dynamics of disorder might account for the opposite behavior between our results and others'. This explanation is consistent with the temperature dependence of the coupling constant. As described in Schmid's theory [46,47], the e-p scattering is suppressed by dynamic disorder. The resultant energy relaxation rate $\tau_{\rm e-p}^{-1}$ is of the order of $(q_T l)\tau_0^{-1}$ where $\tau_0^{-1} \propto T^3$ is the relaxation rate in pure material, q_T is the wave vector of a thermal phonon, and l is the electron mean free path. As $q_T \propto T_{\rm ph}$, the relaxation rate increases with $T_{\rm ph}$.

It is also worthy to note that charge impurities are long-range potentials that preserve the sublattice symmetry. This is in contrast to vacancies, which are short-range potentials and break the sublattice symmetry. The theory for supercollision models disorder as short-range potential [18], while in [17], disorder potential is long ranged. This character of disorder strongly affects scattering of chiral electrons in graphene. Our samples represent a graphene system that is quite different from what is commonly seen, in that dynamic and short-ranged potentials dominate. Therefore, the quantitative understanding of our experimental results, including the power index δ, relies on future theory that takes into account both the dynamics and the symmetry of disorder.

IV. CONCLUSION

In conclusion, we have observed significant suppression of electronic cooling in defected graphene. The cooling power of both monolayer and bilayer graphene samples show $T_{\rm e}^3$ dependence, consistent with disorder-modified electron-phonon coupling in graphene [17,18]. However, the magnitude of the cooling power is over an order of magnitude smaller than that of clean graphene predicted by theory [9,12] and also less than other experiments [35,37]. The suppression of electronic cooling may be related to the dynamic nature of vacancies, which has not been studied in graphene. This effect can be utilized to further improve the performance of graphene-based bolometer and photodetector devices.

ACKNOWLEDGMENTS

This work was supported by National Key Basic Research Program of China (Grants No. 2012CB933404 and No. 2013CBA01603) and NSFC (Projects No. 11074007, No. 11222436, and No. 11234001).

[1] X. Xu, N. M. Gabor, J. S. Alden, A. M. van der Zande, and P. L. McEuen, Nano Lett. **10**, 562 (2009).
[2] N. M. Gabor, J. C. W. Song, Q. Ma, N. L. Nair, T. Taychatanapat, K. Watanabe, T. Taniguchi, L. S. Levitov, and P. Jarillo-Herrero, Science **334**, 648 (2011).
[3] N. G. Kalugin, L. Jing, W. Bao, L. Wickey, C. D. Barga, M. Ovezmyradov, E. A. Shaner, and C. N. Lau, Appl. Phys. Lett. **99**, 013504 (2011).
[4] D. Sun, G. Aivazian, A. M. Jones, J. S. Ross, W. Yao, D. Cobden, and X. Xu, Nat. Nanotechnol. **7**, 114 (2012).
[5] J. Yan, M.-H. Kim, J. A. Elle, A. B. Sushkov, G. S. Jenkins, M. H. M., M. S. Fuhrer, and H. D. Drew, Nat. Nanotechnol. **7**, 472 (2012).
[6] H. Vora, P. Kumaravadivel, B. Nielsen, and X. Du, Appl. Phys. Lett. **100**, 153507 (2012).
[7] K. Yan, D. Wu, H. Peng, L. Jin, Q. Fu, X. Bao, and Z. Liu, Nat. Commun. **3**, 1280 (2012).
[8] X. Cai, A. B. Sushkov, R. J. Suess, M. M. Jadidi, G. S. Jenkins, L. O. Nyakiti, R. L. Myers-Ward, S. Li, J. Yan, D. K. Gaskill *et al.*, Nat. Nanotechnol. **9**, 814 (2014).
[9] S. S. Kubakaddi, Phys. Rev. B **79**, 075417 (2009).
[10] R. Bistritzer and A. H. MacDonald, Phys. Rev. Lett. **102**, 206410 (2009).
[11] W.-K. Tse and S. Das Sarma, Phys. Rev. B **79**, 235406 (2009).
[12] J. K. Viljas and T. T. Heikkilä, Phys. Rev. B **81**, 245404 (2010).
[13] A. C. Betz, F. Vialla, D. Brunel, C. Voisin, M. Picher, A. Cavanna, A. Madouri, G. Fève, J.-M. Berroir, B. Plaçais *et al.*, Phys. Rev. Lett. **109**, 056805 (2012).
[14] A. M. R. Baker, J. A. Alexander-Webber, T. Altebaeumer, and R. J. Nicholas, Phys. Rev. B **85**, 115403 (2012).
[15] A. M. R. Baker, J. A. Alexander-Webber, T. Altebaeumer, S. D. McMullan, T. J. B. M. Janssen, A. Tzalenchuk, S. Lara-Avila, S. Kubatkin, R. Yakimova, C.-T. Lin *et al.*, Phys. Rev. B **87**, 045414 (2013).
[16] F. T. Vasko and V. V. Mitin, Phys. Rev. B **84**, 155445 (2011).
[17] W. Chen and A. A. Clerk, Phys. Rev. B **86**, 125443 (2012).
[18] J. C. W. Song, M. Y. Reizer, and L. S. Levitov, Phys. Rev. Lett. **109**, 106602 (2012).
[19] E. McCann, K. Kechedzhi, V. I. Fal'ko, H. Suzuura, T. Ando, and B. L. Altshuler, Phys. Rev. Lett. **97**, 146805 (2006).
[20] K. Nomura and A. H. MacDonald, Phys. Rev. Lett. **98**, 076602 (2007).
[21] X. S. Wu, X. B. Li, Z. M. Song, C. Berger, and W. A. de Heer, Phys. Rev. Lett. **98**, 136801 (2007).
[22] A. C. Betz, S. H. Jhang, E. Pallecchi, R. Ferreira, G. Feve, J.-M. Berroir, and B. Placais, Nat. Phys. **9**, 109 (2013).
[23] M. W. Graham, S.-F. Shi, D. C. Ralph, J. Park, and P. L. McEuen, Nat. Phys. **9**, 103 (2013).
[24] T. V. Alencar, M. G. Silva, L. M. Malard, and A. M. de Paula, Nano Lett. **14**, 5621 (2014).
[25] A. C. Ferrari, J. C. Meyer, V. Scardaci, C. Casiraghi, M. Lazzeri, F. Mauri, S. Piscanec, D. Jiang, K. S. Novoselov, S. Roth *et al.*, Phys. Rev. Lett. **97**, 187401 (2006).
[26] J. Chen, T. Shi, T. Cai, T. Xu, L. Sun, X. Wu, and D. Yu, Appl. Phys. Lett. **102**, 103107 (2013).
[27] Q. Han, T. Gao, R. Zhang, Y. Chen, J. Chen, G. Liu, Y. Zhang, Z. Liu, X. Wu, and D. Yu, Sci. Rep. **3**, 3533 (2013).
[28] See Supplemental Material at http://link.aps.org/supplemental/10.1103/PhysRevB.91.121404 for resistance of a bilayer graphene and detailed thermal model analysis.
[29] N. Mott, J. Non-Cryst. Solids **1**, 1 (1968).
[30] I. V. Borzenets, U. C. Coskun, H. T. Mebrahtu, Y. V. Bomze, A. I. Smirnov, and G. Finkelstein, Phys. Rev. Lett. **111**, 027001 (2013).
[31] M. S. Fuhrer, Physics **3**, 106 (2010).
[32] Q. Li, E. H. Hwang, and S. Das Sarma, Phys. Rev. B **84**, 115442 (2011).
[33] Y. Zhang, V. W. Brar, C. Girit, A. Zettl, and M. F. Crommie, Nat. Phys. **5**, 722 (2009).
[34] J.-H. Chen, C. Jang, S. Xiao, M. Ishigami, and M. S. Fuhrer, Nat. Nanotechnol. **3**, 206 (2008).
[35] K. C. Fong, E. E. Wollman, H. Ravi, W. Chen, A. A. Clerk, M. D. Shaw, H. G. Leduc, and K. C. Schwab, Phys. Rev. X **3**, 041008 (2013).
[36] The relative contribution of diffusion cooling will increase when e-p coupling is suppressed. It leads to an overestimation of the coupling constant A (see Supplemental Material for details).
[37] R. Somphonsane, H. Ramamoorthy, G. Bohra, G. He, D. K. Ferry, Y. Ochiai, N. Aoki, and J. P. Bird, Nano Lett. **13**, 4305 (2013).
[38] J. Bardeen and W. Shockley, Phys. Rev. **80**, 72 (1950).
[39] C. Herring and E. Vogt, Phys. Rev. **101**, 944 (1956).
[40] H. Suzuura and T. Ando, Phys. Rev. B **65**, 235412 (2002).
[41] N. M. R. Peres, F. Guinea, and A. H. Castro Neto, Phys. Rev. B **73**, 125411 (2006).
[42] J. Rammer and A. Schmid, Phys. Rev. B **34**, 1352 (1986).
[43] C. Y. Wu, W. B. Jian, and J. J. Lin, Phys. Rev. B **57**, 11232 (1998).
[44] W. Jan, G. Y. Wu, and H.-S. Wei, Phys. Rev. B **64**, 165101 (2001).
[45] J. T. Karvonen, L. J. Taskinen, and I. J. Maasilta, Phys. Rev. B **72**, 012302 (2005).
[46] A. Schmid, Z. Phys. **259**, 421 (1973).
[47] A. Sergeev and V. Mitin, Phys. Rev. B **61**, 6041 (2000).
[48] J. J. Lin and J. P. Bird, J. Phys.: Condens. Matter **14**, R501 (2002).
[49] Y. L. Zhong, J. J. Lin, and L. Y. Kao, Phys. Rev. B **66**, 132202 (2002).
[50] A. Pippard, Philos. Mag. Series 7 **46**, 1104 (1955).
[51] S. Adam, E. H. Hwang, V. M. Galitski, and S. Das Sarma, Proc. Natl. Acad. Sci. USA **104**, 18392 (2007).
[52] J. H. Chen, C. Jang, S. Adam, M. S. Fuhrer, E. D. Williams, and M. Ishigami, Nat. Phys. **4**, 377 (2008).